NREL/TP-257-4510 • UC Category: 261 • DE92001157

Dynamic Stall on Wind Turbine Blades

C.P. Butterfield
A.C. Hansen
D. Simms
G. Scott

Prepared for Windpower '91 Conference and Exposition, Palm Springs, California, September 24-27, 1991

National Renewable Energy Laboratory
(formerly the Solar Energy Research Institute)
1617 Cole Boulevard
Golden, Colorado 80401-3393
A Division of Midwest Research Institute
Operated for the U.S. Department of Energy
under Contract No. DE-AC02-83CH10093

December 1991

On September 16, 1991, the Solar Energy Research Institute was designated a national laboratory, and its name was changed to the National Renewable Energy Laboratory.

NOTICE

Printed in the United States of America
Available from:
National Technical Information Service
U.S. Department of Commerce
5285 Port Royal Road
Springfield, VA 22161

Price: Microfiche A01
Printed Copy A02

Codes are used for pricing all publications. The code is determined by the number of pages in the publication. Information pertaining to the pricing codes can be found in the current issue of the following publications which are generally available in most libraries: *Energy Research Abstracts (ERA)*; *Government Reports Announcements* and Index (*GRA* and I); *Scientific and Technical Abstract Reports (STAR)*; and publication NTIS-PR-360 available from NTIS at the above address.

DYNAMIC STALL ON WIND TURBINE BLADES

C.P. Butterfield (NREL*)
A.C. Hansen (University of Utah)
D. Simms (NREL)
G. Scott (NREL)

* National Renewable Energy Laboratory (NREL),
formerly the Solar Energy Research Institute (SERI)

Presented at the Windpower 91' Conference
Palm Springs, CA.
September, 26-28, 1991

Abstract

Dynamic loads must be predicted accurately in order to estimate the fatigue life of wind turbines operating in turbulent environments. Dynamic stall contributes to increased dynamic loads during normal operation of all types of horizontal-axis wind turbines (HAWTs). This reports illustrates how dynamic stall varies throughout the blade span of a 10 m HAWT during yawed and unyawed operating conditions. Lift, drag, and pitching moment coefficients during dynamic stall are discussed. Resulting dynamic loads are presented, and the effects of dynamic stall on yaw loads are demonstrated using a yaw loads dynamic analysis (YAWDYN).

Terminology

C_L	Lift Coefficient
C_{pD}	Pressure Drag Coefficient
C_{Pm}	Pitching Moment Coefficient
C_N	Normal Force Coefficient
C_T	Tangent Force Coefficient
C_{Lmax}	Maximum Lift Coefficient
AOA	Angle of Attack (degrees)

Introduction

Wind turbines are subjected to dynamic loading from a variety of different sources. Wind shear and turbulence cause time-varying inflow that results in unsteady airloads. Tower shadow, upwind turbine wakes, and yaw angles also introduce unsteady inflow to wind turbine rotors. Wind turbine designers must predict these loads in order to adequately design blades, hubs, and the remaining support structure to achieve a 30-year life. Structural analysts have not been able to predict mean or dynamic loads accurately enough to predict the fatigue life of major wind turbine components with confidence. Part of the problem is due to uncertainty in the stochastic wind environment as mentioned earlier. Another important part of the problem is the lack of basic knowledge of rotary wing airfoil stall performance. The helicopter industry has invested significant research time in understanding dynamic stall on helicopter blades but has ignored steady stall because helicopters avoid operating conditions that would result in large-scale steady stall. Wind turbines commonly operate in steady stall as a means of regulating peak power and loads. It has been discovered by Butterfield et al. [1] and many others [2,3] that airfoils do not stall on rotating wings as they do in wind tunnel tests. Butterfield et al. [4] also discovered that dynamic stall can exist on wind turbine blades during normal operating conditions. There is mounting evidence that dynamic stall may be related dynamic loads that are greater than predicted. Wright [5] and Hansen [6] show improved accuracy in predicted dynamic loads and yaw loads when dynamic stall is introduced into their dynamic analyses.

In order to develop static and dynamic stall models for wind turbines, a data base of measured dynamic stall characteristics must exist for comparison and validation of new codes. Helicopter experience and codes may be applicable but must be validated using measurements from operating wind turbine measurements. The Solar Energy Research Institute (SERI), supported by the U.S. Department of Energy (DOE), has conducted a series of experiments that will supply this basic data. The experiment is called the Combined Experiment and is described by Butterfield et al. in two references [7,8]. This paper describes dynamic stall measurements at four blade spanwise stations of a rotating wind turbine blade. Loads are correlated with the measured airloads. Finally, dynamic stall is related to increased yaw moments.

Test Description

A 10-m, three-bladed, downwind horizontal-axis wind turbine (HAWT) was used as a test platform. Molds were made to high tolerances so that airfoil coordinates would be accurately transferred to the test blades. The SERI S809 airfoil was used because extensive wind tunnel data were available for it.

This airfoil is one of a family of airfoils designed specifically for wind turbine use. Tangler and Somers [9,10] describe the airfoil as a 21% thick, laminar-flow airfoil with low roughness sensitivity.

Two blades were made with no instrumentation and a third was constructed with 124 pressure taps installed inside the blade. Butterfield et al. [7] describe the installation technique and the pressure measurement instrumentation. Measurements were made at four chordwise pressure distributions located at 30%, 47%, 63%, and 80% blade spans. Pressure taps were located at 4% chord and 36% chord on the suction side of the airfoil for six additional spanwise locations. Figure 1 shows the wind turbine and basic statistics. Figure 2 shows the pressure tap spanwise locations on the blade and the tap chordwise locations on the airfoil for each of the four spanwise locations.

Four ESP-32 pressure transducers were installed inside the test blade near the chordwise-distributed taps. Stainless-steel tubes were fabricated into the blade skin to carry the surface pressures to each of the transducers. The tube lengths ranged from 4 cm to 7.4 cm and had a 1-mm inside diameter. A microprocessor-based controller was used to electrically scan each of the transducers at a tap-to-tap frequency of 16,672 Hz. Thus each pressure channel was sampled at 521 Hz. Analog filters, set at 100 Hz, were used to prevent aliasing. Transfer functions were measured for each pressure channel to determine the electrical and acoustical dynamic characteristics. In all cases the dynamic response was flat in the region of interest.

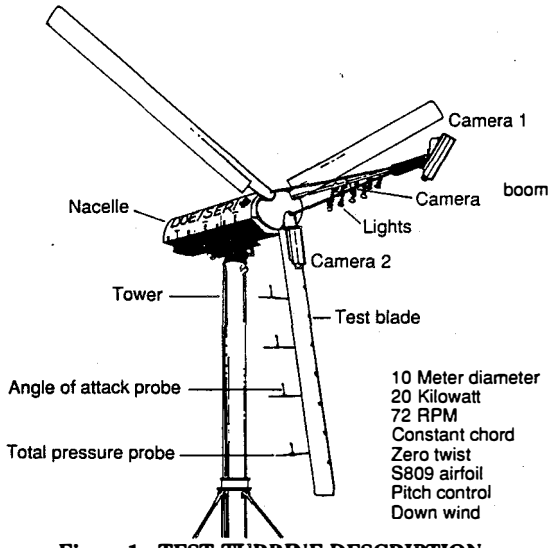

Figure 1. TEST TURBINE DESCRIPTION

The same pressure tap locations and instrumentation were used in wind tunnel tests at the Ohio State University (OSU) [11] and Colorado State University (CSU) [12] wind tunnels. By keeping the instrumentation, pressure tap location, and airfoil identical between wind tunnel tests and rotating blade wind turbine tests, differences in the results would be more likely attributable to real differences in airfoil performance caused by three-dimensional and rotating-blade effects.

Dynamic pressure and local flow angle were measured at each of the four pressure distributions. Dynamic pressure was measured using a total pressure probe with an internal angle of 45 degrees. This probe was tested in the CSU wind tunnel and found to give accurate total pressure measurements for angular misalignments up to 40 degrees. The flow angle probe was also tested in the wind tunnel while mounted on the airfoil. Upwash due to circulation effects causes local flow angles to deviate from the geometric angle of attack. In this test the deviations were measured and used to correct the rotating-blade measured angles. Butterfield et al. [4,1] describes these corrections as well as dynamic response tests performed on the probe.

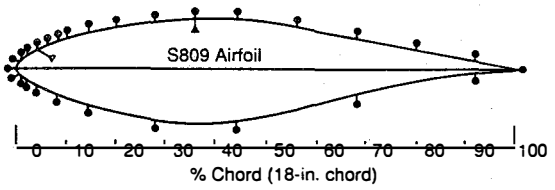

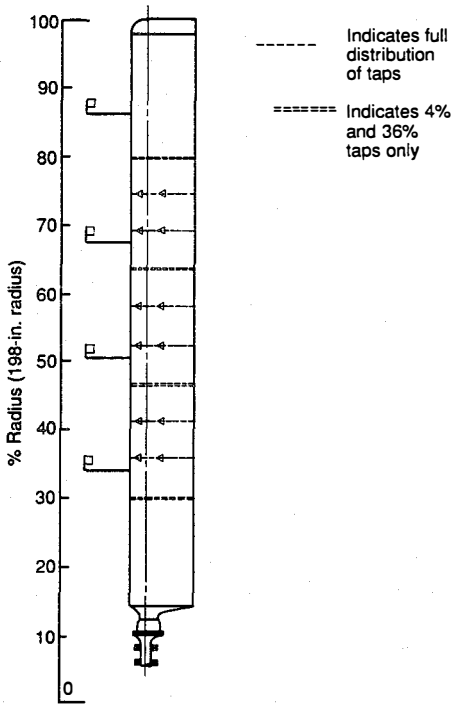

Figure 2. BLADE LAYOUT

Data Case Descriptions

Two data cases were chosen for analysis. The first case spanned 20 seconds of time during 30-degree yaw angle operation and wind speeds of 13.5 m/s. The compass yaw angle of the turbine was 300 degrees while the wind direction was 270 degrees. The turbine rotates clockwise when viewed from a downwind location looking into the wind. The instrumented blade is pointing up when in the zero degree azimuth position.

The second case spanned 10 seconds of time during zero yaw error in wind speeds of 15 m/s. These two cases are compared in Table 1 and were chosen to illustrate the conditions which cause dynamic stall.

The yawed case is typical of conditions that normally occur during rapid wind direction changes for yaw-driven or free yaw HAWTs. Yaw-driven wind turbines respond to wind direction changes at yaw rates less than one to five degrees per second. The low yaw rates are chosen to limit gyroscopic loads on the main shaft, which are far greater than unsteady aerodynamic loads if allowed to yaw freely. Wind direction changes occur at much higher rates and result in 30- to 40-degree yaw errors while the turbine is catching up with the wind direction change.

Free yaw machines with ridged rotors respond at higher yaw rates but will experience yaw errors during yaw overshoot. Free yaw machines with teetered or soft rotors will respond to wind direction changes at lower yaw rates that are over-damped. This damped response still results in yaw errors, but yaw rates are reduced, which results in reduced gyroscopic loads.

TABLE 1

	30° Yaw Case	No Yaw Case
VPA Ave. Wind Speed (m/s)	13.67	15.39
Ave. Turb. Intensity	0.14	0.06
Shear (m/s)	1.24	0.72
Pitch Angle (degree)	11.3	11.54
Pitch Std. Dev. (degree)	0.33	0.21.
Rotor Torq. (N-m)	1392	1976

Azimuth Averaged Results

Figures 3 through 6 illustrate angle of attack (AOA) and lift coefficient (C_L) variations azimuth averaged over 25 revolutions during 30-degree yawed operation for 80%, 63%, 47%, and 30% blade spans. The inboard stations clearly reach high values of C_{Lmax} while the blade is rising at azimuth angles of 270 degrees. Minimum values of C_L occur after the airfoil has stalled, when the blade azimuth angle is between 0 and 90 degrees, on the down-wind side of the rotor. Static stall in wind tunnel tests results in values of C_{Lmax} equal to 0.95. If the airfoil did not stall and was linearly related to AOA, the C_L would follow the AOA in the cosine shape shown in the same figures. The difference in lift that exists from the upwind side of the yawed rotor (200 to 300 degree azimuth angle) to the down wind side of the rotor (0 to 100 degree azimuth angle) causes high yaw moments and low speed shaft (LSS) cyclic loads.

Peak-to-peak values of AOA vary from 11 degrees, at the 80% span to 26 degrees at the 30% span. This implies that all horizontal-axis rotors would experience AOA cyclic amplitudes large enough to cause dynamic stall for even modest yaw angles. Both fixed-pitch rotors and partially feathered pitch-control rotors would experience maximum AOAs great enough to cause local stalling.

Figures 7 through 10 show similar plots of C_L and AOA variations during 0 degree yaw error operation. As can be seen for this case, AOA variations are small by comparison because asymmetrical inflow is due only to wind shear of 0.7 m/s across the rotor. Tower shadow is the major contributor to inflow disturbances. This is obvious from the rapid change in AOA and C_L at 180 degree azimuth angle. This disturbance is large enough to cause dynamic stall as implied by the sudden rise in C_L above static stall C_{Lmax} of 0.95.

Dynamic Stall Results

Figures 11 through 14 illustrate azimuth-averaged C_L vs. AOA compared to static lift curves measured in the CSU wind tunnel tests [12]. The dynamic stall behavior is evident in the large hysteresis loops that surround the static curves. At the 80% span the rotating blade C_{Lmax} values do not exceed static values significantly. Conversely, Figures 12 through 14 show stations 63%, 47%, and 30%, which show C_{Lmax} values exceeding static values by 32% to 110% respectively. The labeled center symbols indicate blade azimuth angle. The difference in lift at azimuth angles of 90 degrees and 270 degrees is again obvious in these curves. As the hysteresis loops grow larger, the differences increase and the resulting yaw moments increase.

Drag is also subject to the effects of dynamic stall. Figures 15 through 18 compare dynamic stall measurements during 30-degree yawed opera-

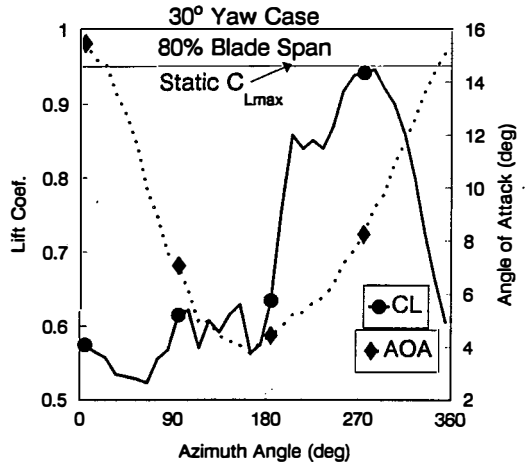

Figure 3. AZIMUTH AVERAGED AOA AND LIFT COEF. AT 80% SPAN FOR 30 DEGREE YAW CASE

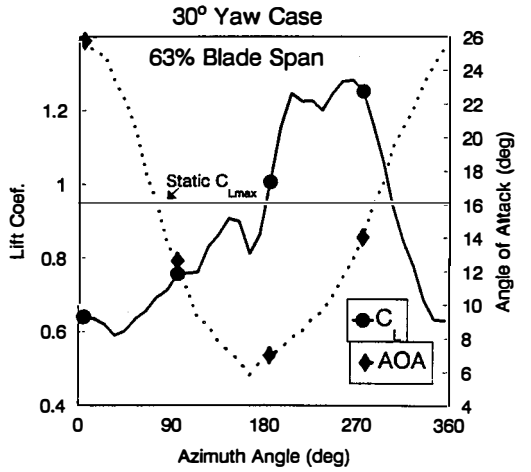

Figure 4. AZIMUTH AVERAGED AOA AND LIFT COEF. AT 63% SPAN FOR 30 DEGREE YAW CASE

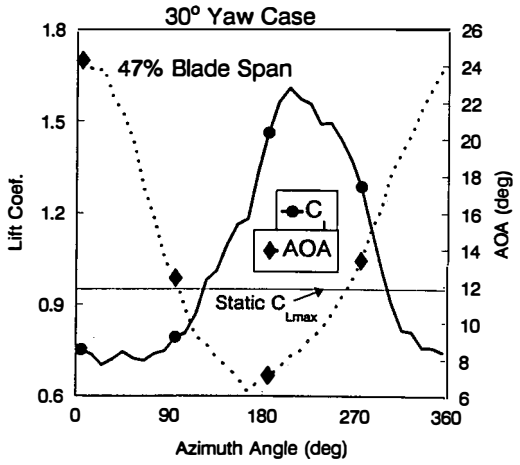

Figure 5. AZIMUTH AVERAGED AOA AND LIFT COEF. AT 47% SPAN FOR 30 DEGREE YAW CASE

tion with static data from the CSU wind tunnel. The 80% span is affected minimally, but inboard stations experience nearly double the drag from one side of the rotor to the other. Figure 16 shows a C_{pD} at 270 degree azimuth angle of 0.15 and at 90 degree 0.07, more than a factor of two increase. These differences will also contribute to yaw moments during yawed operation.

Pitching moment coefficients also experience dynamic stall. Figure 19 shows C_{Pm} hysteresis loops measured at the 63% blade span. These moments can have a significant effect on blade pitch angle if flexibility exists in the pitch linkage of pitch-control rotors.

Two-dimensional dynamic-stall tests have been conducted by Gregorek et al. [11] in the OSU 3X5 wind tunnel. Figure 12 compares Gregorek's two-dimensional dynamic-stall data with those measured on the operating turbine during 30-degree yawed operation. Wind tunnel data show only 11% increases in C_{Lmax} over wind tunnel values of C_{Lmax}. This may be due in part to the smaller AOA amplitudes used in these tests. The OSU data shown include three separate tests. Each test had a +/- 3-degree amplitude with 2-degree, 8-degree and 15-degree mean values of AOA. Spanwise flow effects in separated flow regions may also contribute higher values of C_{Lmax} measured on the rotating blade data. Future dynamic stall tests will be run at higher amplitudes to investigate the cause of this discrepancy.

Loads

During yawed operation cyclic airloads cause cyclic blade loads. Figure 20 illustrates these blade loads correlated with airloads at the 63% blade span. Peak blade loads correlate with peak lift forces. Blade loads from all three blades sum together and result in hub loads. Any imbalances in blade loads result in LSS moments and yaw moments. Figure 21 illustrates measured yaw moments during 30-degree yawed operation. The cyclic moment is due to each blade reaching maximum load at different rotor azimuthal positions. As shown in Figure 21 one yaw peak correlates with the instrumented blade reaching maximum lift force.

Blade stalling effects yaw loads because the blade reaches maximum lift on one side of the rotor and minimum lift on the opposite side of the rotor. Dynamic stall dramatically increases yaw loads because C_{Lmax} overshoot increases the difference between maximum airload on one side of the rotor and minimum airload on the opposite side of the rotor. This can be demonstrated by running the YAWDYN simulation analysis with and without dynamic stall. This analysis was developed and validated by Hansen et al. [6].

Figure 22 shows how predicted yaw moments compare with measured yaw moments. The three-per-revolution (3P) components of the predictions appear to be 75% greater than the measured 3P component. They also appear to be in phase by 60 degrees. The mean values of measured loads are 30% greater than the predicted values with dynamic stall included. This discrepancy may be due to the over-simplified dynamic stall model used in this analysis. If dynamic stall is excluded from the analysis the mean yaw moment drops to one half of that predicted using a simple dynamic-stall model. This difference is dramatic, especially when considering the dynamic stall model used did not include C_{Lmax} overshoot, only hysteresis. If accurate values of C_{Lmax} were used throughout the blade span, even larger yaw moments would be predicted. A more accurate yaw model may also explain the discrepancy between the measured yaw moments and predicted moments.

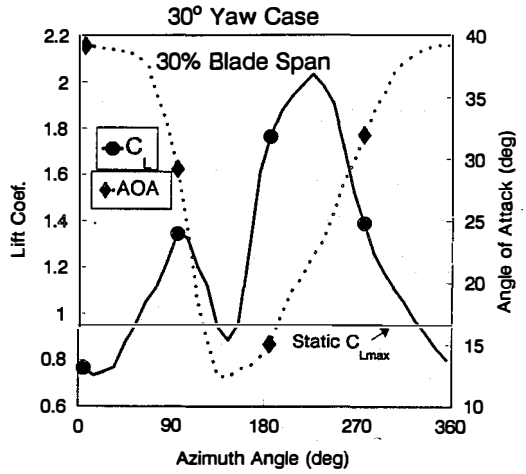

Figure 6. AZIMUTH AVERAGED AOA AND LIFT COEF. AT 30% SPAN FOR 30 DEGREES YAW CASE

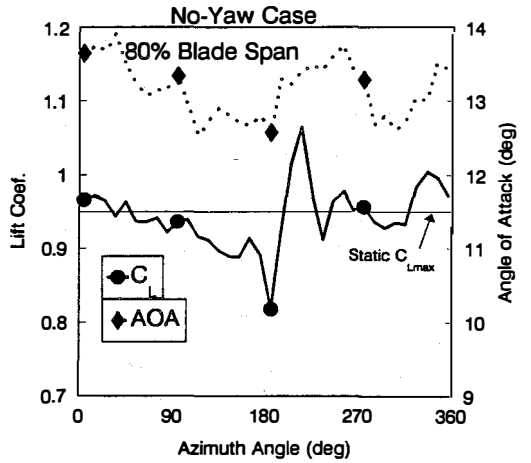

Figure 7. AZIMUTH AVERAGED AOA AND LIFT COEF. AT THE 80% SPAN FOR NO YAW CASE

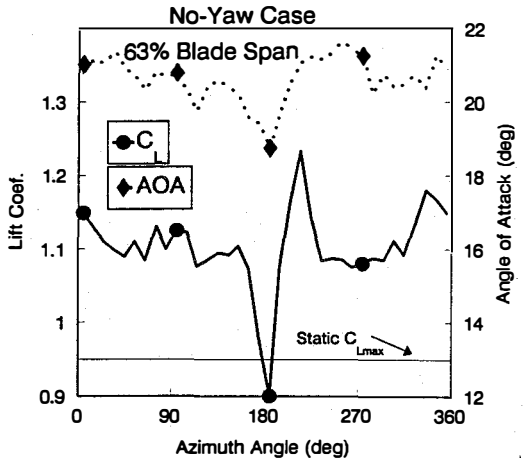

Figure 8. AZIMUTH AVERAGED AOA AND LIFT COEF. AT 63% SPAN FOR NO YAW CASE

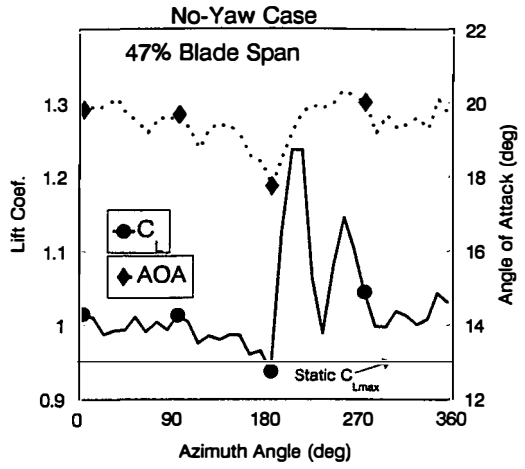

Figure 9. AZIMUTH AVERAGED AOA AND LIFT COEF. AT 47% SPAN FOR NO YAW CASE

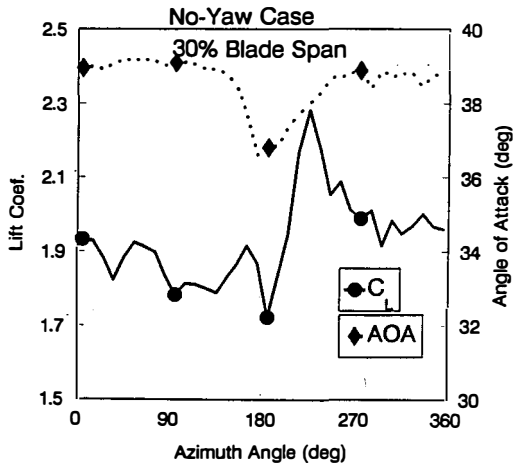

Figure 10. AZIMUTH AVERAGED AOA AND LIFT COEF. AT 30% SPAN FOR NO YAW CASE

Conclusions

Dynamic stall was shown to exist on a HAWT operating at 30-degree yaw angle. Dynamic stall also occurs for low yaw error operation when tower shadow, wind shear, or inflow turbulence cause large AOA excursions. These increased aerodynamic loads cause increased structural loading. Yaw moments are affected by dynamic stall.

Future work

Blade geometry appears to effect airfoil performance. To understand the effect of blade twist and taper on airfoil stall performance, a tapered and twisted blade, will be developed and tested. Results will be compared to the existing blade which has no twist or taper.

The flow conditions adjacent to the blade but off the surface (outer flow condition) may reveal the cause of airfoil performance abnormality. These flow states can be tested by observing smoke flow patterns as the blade is rotating through the smoke. Video cameras will be used to record these smoke patterns. Video image processing will be used to correlate the patterns with pressure distributions and other operating conditions. This information will be used to improve stall models for wind turbines.

Acknowledgments

This work was conducted with the support of the DOE under contract DE-AC02-83CH10093. Many others have contributed to the success of this program. RANN Inc. has offered guidance in the basic science of aerodynamics. Ohio State University has offered wind tunnel testing and instrumentation design assistance. SERI colleges have been a constant source of guidance and assistance. Walt Musial conducted most of the tests and has provided valuable advise. Bob Thresher has provided invaluable support and technical guidance.

References

1. Butterfield, C.P., D.A. Simms, W.P. Musial, G.N. Scott, Spanwise Aerodynamic Loads on a Rotating Blade, SERI/TP-257-3983, UC Category:261, DE91002101 (Wind Power 90', October 1990).

2. Musial, W., and C.P. Butterfield, A Comparison of Two- and Three-Dimensional S809 Airfoil Properties for Rough and Smooth HAWT Rotor Operation, SERI/TP-257-3603, UC Category: 261, DE89009512 (ASME Jan. 1990).

3. Viterna, L.A., and R.D. Corrigan, Fixed Pitch Rotor Performance of Large Horizontal Axis Wind Turbines, DOE/NASA Work-shop on Large Horizontal Axis Wind Turbines, (Cleveland, Ohio), July 28-30, 1981.

4. Butterfield, C.P., Three-Dimensional Airfoil Performance Measurements on a Rotating Wing, SERI/TP-217-3505, Solar Energy Research Institute, Golden, CO (June 1989).

5. Wright, A., and C.P. Butterfield, The SERI Teetering Hub Rotor Code: Final Results and Conclusions, Wind Power 91, Palm Springs, CA. September 1991.

6. Hansen, A.C., C.P. Butterfield, "Yaw Loads and Motions of a Horizontal Axis Wind Turbine", ASME Journal of Solar Energy, November, 1990, Vol 112.

7. Butterfield, C.P., and E. Nelson, Aerodynamic Testing of a Rotating Wind Turbine Blade, SERI/TP-257-3490, Solar Energy Research Institute, Golden, CO (January 1990)

8. Butterfield, C.P., M. Jenks, D. Simms, W. Musial, Aerodynamic Pressure Measurements on a Rotating Wind Turbine Blade, SERI/TP-257-3695, Solar Energy Research Institute, Golden, CO (May 1990).

9. Tangler, J., D. Somers, Status of the Special Purpose Airfoil Families, SERI/TP-217-3264, Solar Energy Research Institute, Golden, CO (December 1987).

10. Somers, D.M., Design and Experimental Results for the S809 Airfoil, March 1989 (to be published)

11. Gregorek, G.M. (unpublished report of OSU testing of S809 Nov. 1989).

12. Butterfield, C.P., G. Scott, W. Musial, Comparison of Wind Tunnel Airfoil Performance Data with Wind Turbine Blade Data, SERI/TP-254-3799, Solar Energy Research Institute, Golden, CO (July 1990).

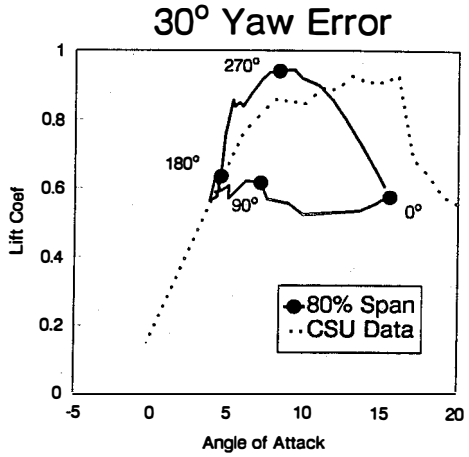

Figure 11. DYNAMIC STALL AT 80% SPAN

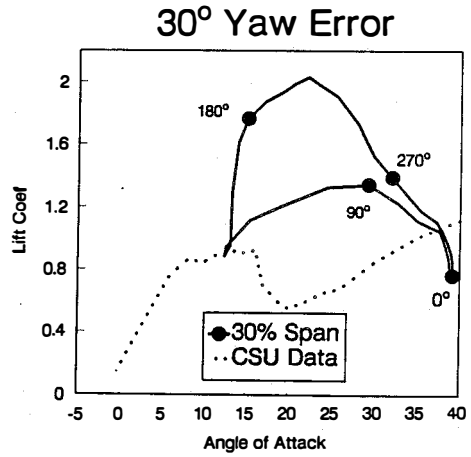

Figure 14. DYNAMIC STALL AT 30% SPAN

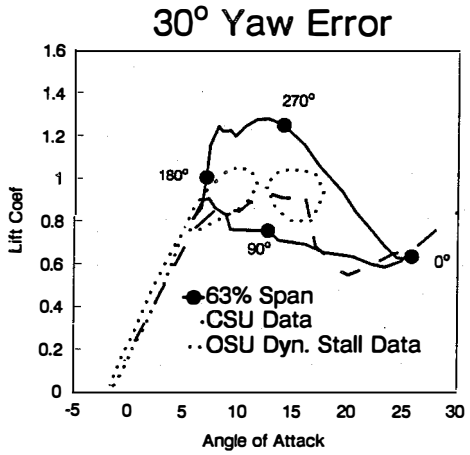

Figure 12. DYNAMIC STALL AT 63% SPAN COMPARED TO WIND TUNNEL DYNAMIC STALL

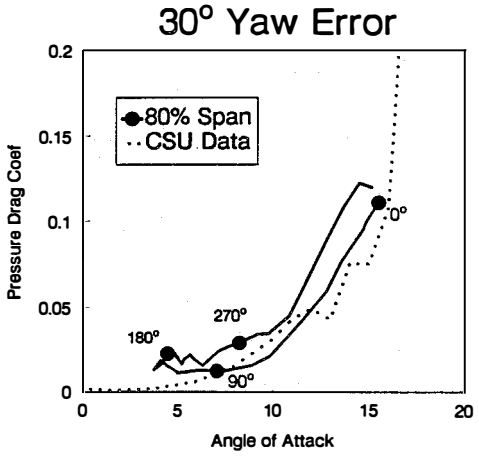

Figure 15. DRAG DYNAMIC STALL AT 80% SPAN

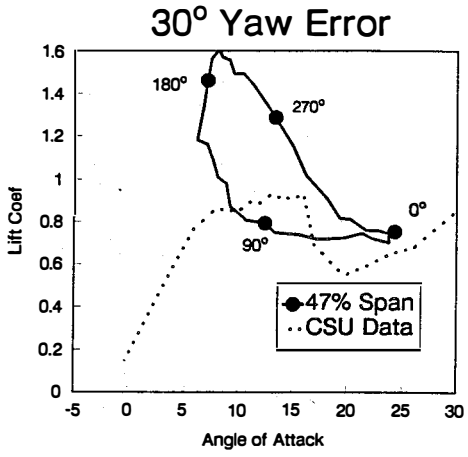

Figure 13. DYNAMIC STALL AT 47% SPAN

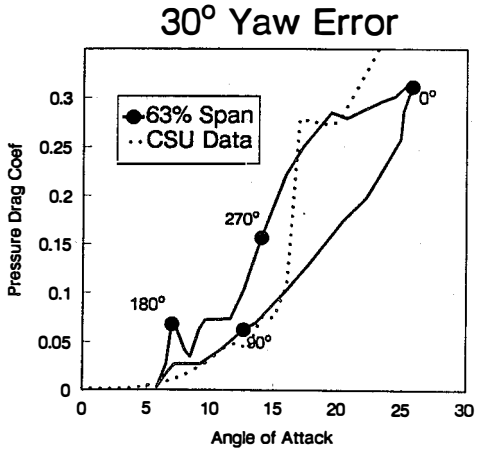

Figure 16. DRAG DYNAMIC STALL AT 63% SPAN

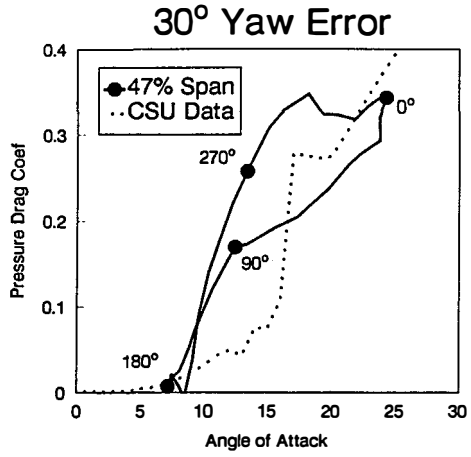

Figure 17. DRAG DYNAMIC STALL AT 47% SPAN

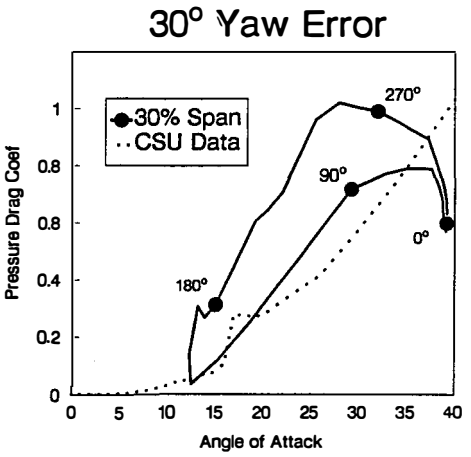

Figure 18. DRAG DYNAMIC STALL AT 30% SPAN

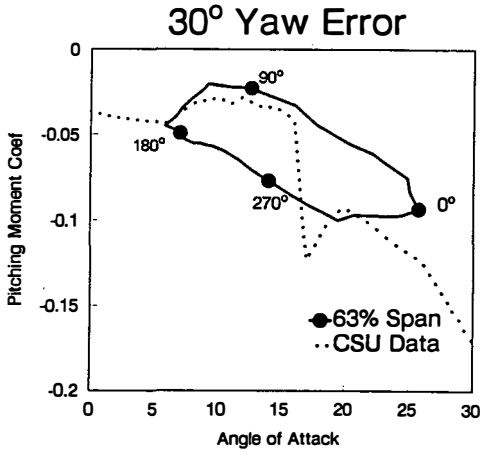

Figure 19. PITCHING MOMENT DYNAMIC STALL AT 63% SPAN

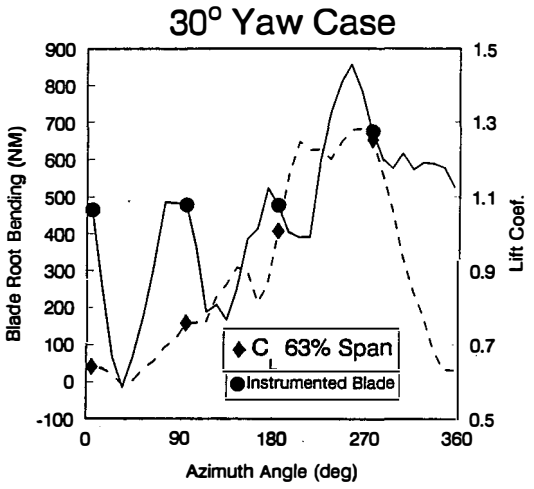

Figure 20. BLADE ROOT LOADS DURING YAWED OPERATION

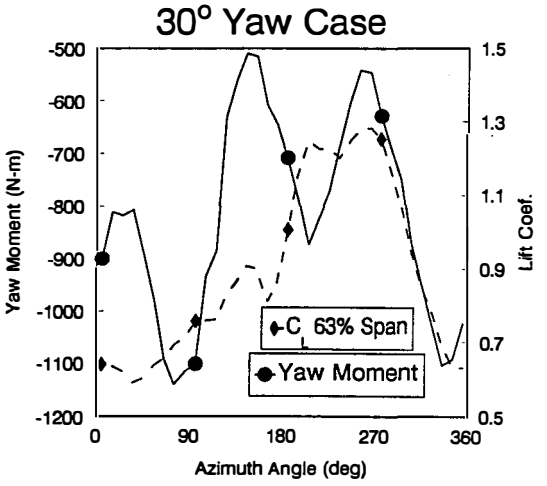

Figure 21. YAW MOMENTS DURING YAWED OPERATION

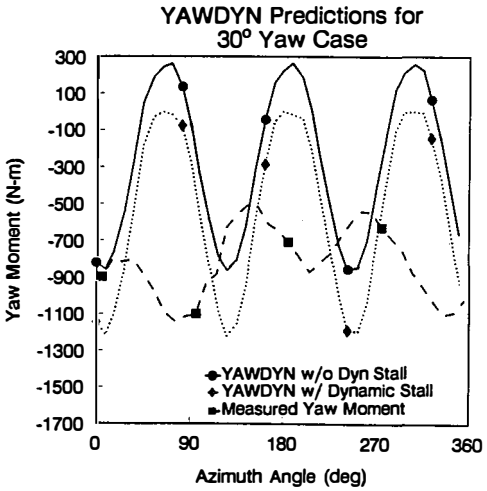

Figure 22. YAW DYN PREDICTION OF YAW MOMENT